Theory overview on electroweak emission from heavy-ion collisions*

Greg Jackson[1,**]

[1]SUBATECH (IMT Atlantique, Nantes Université, IN2P3/CNRS),
4 rue Alfred Kastler, La Chantrerie BP 20722, 44307 Nantes, France

Abstract. An important class of observables in the heavy-ion collision programme concerns probes which are not sensitive to the prevailing strong interactions of QCD. The emission of photons, weak gauge bosons, and leptons fall into this category. Here I will describe the current status of such investigations, focusing on the emerging theoretical picture and its uncertainties.

1 Introduction

For weak probes of strongly interacting systems, the hierarchy $\alpha_{\rm em} \ll \alpha_s$ allows the calculation to be conveniently organised by first expanding the result in $\alpha_{\rm em} = e^2/(4\pi)$. For instance, photons are generated (via $H_{\rm int} = i\,e\,A_\mu J^\mu_{\rm em}$) at a rate given by [1, 2]

$$\Gamma_\gamma \;\sim\; e^2 \left\langle J_{\rm em}\, J_{\rm em} \right\rangle + O(e^4)\,, \tag{1}$$

where the average is calculated from the density matrix $\langle ... \rangle = {\rm Tr}[\,\hat\rho\,(...)\,]$. In heavy-ion collisions the system is too short-lived for photons or other weak probes to equilibrate, so they "escape" basically unmodified, unlike jets or soft hadrons (see refs. [3] and [4] for recent overviews). Produced at all stages and throughout the volume, they are most copious when the medium is hottest, posing the challenge of disentangling the various sources.

The theoretical agenda is twofold. It involves *i*) the microscopic calculation of production rates, as well as *ii*) the macroscopic embedding of those rates in simulations of heavy-ion collisions. Task *i*) requires field theory calculations of eq. (1), such as by expanding in α_s, using effective hadronic or QCD based theories, or from non-perturbative lattice studies. Predictions, e.g. for the $p_{\rm T}$ spectrum of photons and the invariant mass M distribution of dileptons, are obtained from *ii*) by integrating over the spacetime history. This second step must be done numerically using multi-stage frameworks, which typically involve hydrodynamic codes such as MUSIC [5] or *Trajectum* [6].

In these proceedings, I will highlight recent theoretical progress on electroweak probes as presented at the conference. Let me draw attention to the excellent similar reports in refs. [7–10], from the past few years. For an update of experimental developments, see ref. [11]. Here I will focus on photons and dileptons, using a notation where Γ_γ and $\Gamma_{\ell\bar\ell}$ are the respective differential rates per time and volume. The dilepton pair is produced through a virtual photon, of energy $\omega \geq (4m_\ell^2 + \boldsymbol{k}^2)^{1/2}$, where $\boldsymbol{k}$ is the photon's momentum and m_ℓ is the mass of each lepton. For real photons, $\omega = k \equiv |\boldsymbol{k}|$.

*Invited plenary talk at the 31st International Conference on Ultra-relativistic Nucleus-Nucleus Collisions (Quark Matter 2025), Frankfurt, Germany, Apr 6-12, 2025.

**e-mail: jackson@subatech.in2p3.fr

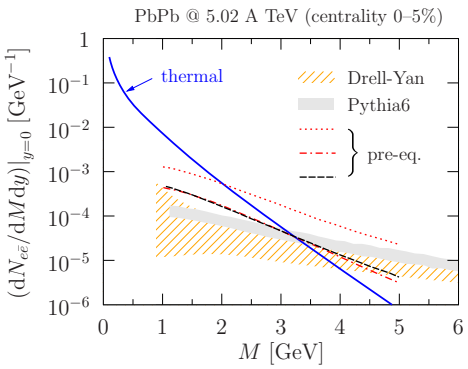

Figure 1. Dielectron yield from the QGP as a function of M, for central PbPb collisions at midrapidity. The thermal component (blue solid) represent NLO+LPM$^{\mathrm{LO}}$ convoluted with hydrodynamics (see fig. 3 of ref. [16]). The pre-equilibrium results include the LO rates in kinetic theory with (red dash-dotted, black dashed) and without (red dotted) initial quark suppression. See ref. [14] (black, event-by-event simulation) and ref. [15] (red, boost invariant evolution) for more details. The NLO Drell-Yan result is shown, as well as a prediction from the Pythia6 event generator.

2 Main stages and their emission rates

A source of electromagnetic probes which is common to both pp and AA collisions, originates from the first instant of the collision where eq. (1) involves the initial hadronic wavefunction of the projectiles. Such photons and dileptons are called *prompt* and can be calculated within the QCD factorization framework, involving the parton distribution functions (PDFs, $f_{i/\mathrm{A}}$ below) [12]. For dileptons this is called the Drell-Yan process, and at leading order (LO) it is [1]

$$\left.\frac{\mathrm{d}N^{\mathrm{DY}}_{\mathrm{AB}\to\ell\bar{\ell}}}{\mathrm{d}M^2\,\mathrm{d}y}\right|_{\mathrm{LO}} = T_{\mathrm{AB}}\,\frac{e^4\sum_i Q_i^2}{36\pi M^2 s}\,f_{i/\mathrm{A}}(x_1)\,f_{\bar{i}/\mathrm{B}}(x_2)\,, \tag{2}$$

the geometric overlap $T_{\mathrm{AB}} = N_{\mathrm{coll}}/\sigma^{\mathrm{inel}}_{\mathrm{pp}}$ is an effective luminosity, the quark charge fractions are $Q_i = \{\frac{2}{3}, -\frac{1}{3}\}$, and nuclear PDFs (per nucleon) are evaluated at the longitudinal momentum fractions $x_{1,2} = Me^{\pm y}/\sqrt{s}$ (y is the rapidity of the dilepton). At higher order in perturbation theory, eq. (2) generalises to a convolution of the nuclear PDFs with a hard scattering kernel and the kinematics is more complicated.[2] The Drell-Yan signal is dominant for large M and allows one to study isospin content (via Q_i), sea quark asymmetry, and possibly the small-x behaviour of nuclear PDFs (at large/small y).

Quite rapidly (within a time $\tau_{\mathrm{eq}} \simeq 1$ fm/c), the longitudinal initial momentum distributions of partonic degrees of freedom approach local thermal equilibrium. Considerable progress in understanding how this occurs has been made with kinetic transport theory. In this approach, Boltzmann equations describe the evolution of quark and gluon distribution functions (denoted $f_{q,\bar{q},g}$ below) and can similarly track photon emission [13]. The rate from $2 \to 2$ processes is

$$\left.\frac{\mathrm{d}\Gamma_\gamma}{\mathrm{d}^3\boldsymbol{k}}\right|_{2\to2} = \frac{1}{4k(2\pi)^3}\sum_{a,b,c}\int \mathrm{d}\Omega_{2\to2}\,f_a\,f_b\,[1\pm f_c]\,|\mathcal{M}_{ab\to c\gamma}|^2\,, \tag{3}$$

where at LO one has $q\bar{q} \to g\gamma$ and $qg \to q\gamma$. Also included are $1 + n \leftrightarrow 2 + n$ processes, as mandated by the Landau-Pomeranchuk-Migdal (LPM) effect. The rate $q\bar{q} \to \gamma^*$ has been used to describe pre-equilibrium dilepton yields.[3] Those yields have a particular scaling in time which involves the viscosity to entropy density ratio [14]. At LHC energies, the initial wavefunction is dominated by gluons and it takes some time to populate the quark and antiquark distributions. This implies a suppression of very early electroweak emissions, which It has been suggested may influence the dilepton invariant mass spectrum [15, 16], see fig. 1.

[1] Equation (2) only includes the γ^* intermediate state, but for large M, the Z boson must also be taken into account.

[2] The formalism introduces a renormalisation scale μ_{R} (e.g. in α_s) and a factorization scale μ_{F} (e.g. in $f_{i/\mathrm{A}}$) which are typically evaluated at $\mu_{\mathrm{R}}, \mu_{\mathrm{F}} = M$. This choice is varied by a factor of 2 to estimate the uncertainty.

[3] Such a LO dilepton rate is similar to eq. (2), with the nPDFs replaced with general distribution functions.

In thermal equilibrium, eq. (1) is evaluated with a thermal density matrix characterized by a temperature T (and chemical potentials). The differential rates are proportional to the vector spectral function, given formally by analytic continuation of the Euclidean correlator:

$$\rho^{\mu\nu}(\omega,\boldsymbol{k}) = -\mathrm{Im}[\int_0^{1/T}\mathrm{d}\tau\; e^{ik_n\tau}G^{\mu\nu}(\tau,\boldsymbol{k})]_{ik_n\to\omega+i0^+}\;; \quad G^{\mu\nu}\equiv\int_{\boldsymbol{x}} e^{-i\boldsymbol{k}\cdot\boldsymbol{x}}\left\langle V^\mu(\tau,\boldsymbol{x})V^\nu(0)\right\rangle \tag{4}$$

where $\int_{\boldsymbol{x}}\equiv\int\mathrm{d}^3\boldsymbol{x}$ and $V^\mu\equiv\bar\psi\gamma^\mu\psi$. The photon and dilepton rates are given, respectively by

$$\frac{\mathrm{d}\Gamma_\gamma}{\mathrm{d}^3\boldsymbol{k}} = \frac{\alpha_{\mathrm{em}}\sum_i Q_i^2}{2\pi^2\,k}n_{\mathrm{B}}(k)\,\rho_{\mathrm{V}}(\omega,\boldsymbol{k})\Big|_{\omega=k} + \mathcal{O}(\alpha_{\mathrm{em}}^2)\,, \tag{5}$$

$$\frac{\mathrm{d}\Gamma_{\ell\bar\ell}}{\mathrm{d}\omega\mathrm{d}^3\boldsymbol{k}} \approx \frac{\alpha_{\mathrm{em}}^2\sum_i Q_i^2}{3\pi^3M^2}n_{\mathrm{B}}(\omega)\,\rho_{\mathrm{V}}(\omega,\boldsymbol{k}) + \mathcal{O}(\alpha_{\mathrm{em}}^3)\,, \qquad \text{where} \quad \rho_{\mathrm{V}}\equiv\rho_\mu{}^\mu\,. \tag{6}$$

Here ω and $\boldsymbol{k}$ are the photon energy and momentum in the medium's local rest frame. However, eqs. (5) and (6) apply cell-by-cell when simulating a heavy ion collision. The temperature $T(t,\boldsymbol{x})$ varies in space and time, while ω and $\boldsymbol{k}$ need to be boosted to the lab frame according to the local fluid velocity $u^\mu(t,\boldsymbol{x})$. Hydrodynamical evolution governs these macroscopic quantities, and hence the observed yields $\mathrm{d}N=\int_{t,\boldsymbol{x}}\mathrm{d}\Gamma$ are sensitive to viscous corrections (as are the rates themselves) [17–19]. New results for finite μ_{B} were presented at the conference [20].

As the system cools and expands, partons confine into a gas of hadrons. Freeze-out ends the thermal phase, and hadrons undergo re-scatterings and resonance decays. It is speculated that the hadronization process may entail photon production [21]. The subsequent hadronic dynamics is usually treated with transport codes (e.g. SMASH or UrQMD), where photons originate from individual scatterings requiring cross sections as input [22]. For lower collisional energies (e.g. the RHIC beam energy scan), the bayon-rich region of the phase diagram is explored. A "cocktail" of hadronic reactions shapes the dilepton invariant mass spectrum [23], and for $M\lesssim 1$ GeV the crucial physics arises from effective hadronic many-body dynamics with strong in-medium modifications. Novel phenomena may occur as μ_{B} increases, e.g. a phase transition (rather than crossover) [24] or a possible "moat" regime [25].

3 Perturbation theory and lattice

The spectral function in eqs. (5) and (6) may be evaluated from first principles either by a weak coupling expansion (in α_s) or by non-perturbative lattice QCD. Much of the phenomenology in sec. 2 is currently based on perturbation theory.[4] In equilibrium, the nature of the strict perturbative calculation of ρ_{V} (which has a long history) depends upon the kinematic domain. To compare with lattice data, the strict NLO result (applicable for $M\gtrsim T$) is combined with the regime of LPM resumation (for $M\sim gT$), see ref. [38]. If $\rho^{\mu\nu}$ is known,

$$G^{\mu\nu}(\tau,\boldsymbol{k}) = \int_0^\infty\mathrm{d}\omega\,\rho^{\mu\nu}(\omega,\boldsymbol{k})\,\cosh[(\tfrac{1}{2T}-\tau)\omega]/(\pi\sinh[\tfrac{\omega}{2T}])\,. \tag{7}$$

The reverse, i.e. extracting the frequency dependence of ρ from measurements of G, is an ill-conditioned operation for which there are a variety of strategies [32]. Studies were first made at zero momentum ($\boldsymbol{k}=0$) [33] and then non-zero momentum [34]. Recent progress enables us to scrutinize pQCD and make quantitative estimates of non-perturbative contributions.[5]

The tensor structure has two independent components, transverse (T) and longitudinal (L) w.r.t. $\boldsymbol{k}$. Aligning the momentum with the z-axis: $\boldsymbol{k}\to k\,\boldsymbol{e}_z$, they can be expressed as $G_{\mathrm{T}}\equiv\frac{1}{2}\sum_{i=1}^2 G^{ii}$ and $G_{\mathrm{L}}\equiv G^{33}-G^{00}$. Another basis is $G_{\mathrm{V}}\equiv 2\,G_{\mathrm{T}}+G_{\mathrm{L}}$ and $G_{\mathrm{H}}\equiv 2\,(G_{\mathrm{T}}-G_{\mathrm{L}})$. For an $N_s^3\times N_\tau$ lattice, the momenta $k=2\pi n/(aN_s)$, where a is the lattice spacing and n is an integer. The correlators are periodic in the imaginary-time direction and symmetric on the interval $\tau\in[0,1/T]$, although cut-off effects are difficult to control for $\tau T\lesssim\frac{1}{4}$.

[4] The fixed value $\alpha_s\approx 0.3$ ($g\approx 2$) is commonly used, although not always stated in the literature.
[5] A different approach, free of the inverse problem, utilises imaginary spatial momenta [39, 40].

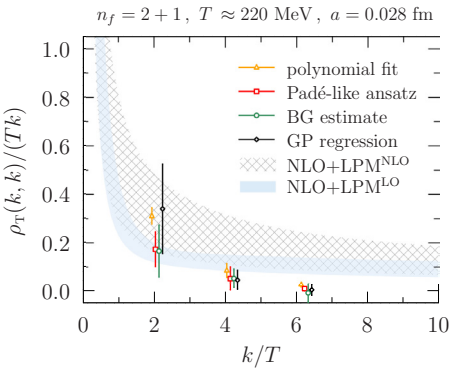

Figure 2. Transverse spectral function at the photon point $\omega = |\boldsymbol{k}|$, obtained from spectral reconstruction methods for $G_{\rm H}$ [37]. Results are shown for simulations on a fixed lattice for $T = 220$ MeV (spacing $a = 0.028$ fm), with an unphysical pion mass of $m_\pi = 320$ MeV. The correlators were measured at $k = T \times 2\pi n/3$, $n = 1, 2, 3$. (Error bars are slightly displaced for better visibility; BG = Bakus-Gilbert; GP = Gaussian Process.) The resummed spectral function from perturbation theory is also shown as a band (which results from the scale variation in α_s) see ref. [38] for details.

Note that for $\omega = k$, the Ward identity implies $\rho^{00} = \rho^{33}$ and hence $\rho_{\rm L} = 0$. Therefore either $G_{\rm V}$ or $G_{\rm H}$ may be analyzed for the photon rate. Dileptons however require $\rho_{\rm V}$ in the timelike domain, where it receives a large contribution $\propto M^2 = \omega^2 - k^2$ from vacuum physics. This reflects itself in $G_{\rm V} \sim 1/\tau^3$ for small τ, making it difficult to constrain the *thermal* information in $\rho_{\rm V}$. On the other hand, $\rho_{\rm H}$ vanishes exactly in vacuum (as well as for $\boldsymbol{k} = 0$) and satisfies the sum rule $\int {\rm d}\omega\, \omega \rho_{\rm H} = 0$. There is now a wealth of information on Euclidean correlators and spectral functions for $T > T_c$ [35–37]. Phenomenological models should therefore be tested on these lattice data before making predictions. So far these studies seem to indicate, see fig. 2, that pQCD alone slightly overestimates the photon rate at large k/T.

4 What we can learn from EM probes

4.1 Temperature of the QGP

The thermal distribution function in eqs. (5) and (6) implies that the integrated rates scale like T^4, i.e. hotter regions radiate the most. For this reason photons and dileptons can act as "thermometers" of the medium. If the measured spectra are approximately exponential, an effective temperature $T_{\rm eff}$ can be defined from the inverse logarithmic slope, e.g. ${\rm d}N_\gamma/({\rm d}y\, p_{\rm T}{\rm d}p_{\rm T}) \propto \exp(-p_{\rm T}/T_{\rm eff})$ and ${\rm d}N_{\ell\bar{\ell}}/({\rm d}y\, {\rm d}M) \propto (MT_{\rm eff})^{3/2} \exp(-M/T_{\rm eff})$. However, as clear from sec. 2, the value of $T_{\rm eff}$ derives from a superposition of sources. It is important to understand which factors control this value, in order to interpret the experimental findings [11]. In the case of photons, $p_{\rm T}$ is blue shifted relative to its value in the local rest frame due to radial flow [6, 47]. For dileptons M is an invariant quantity and the slope parameter is found to correlate with the initial mean temperature in simulations [41–43].

4.2 Electrical conductivity

The limit $\omega, k \ll T$ is one in which charge fluctuations are classical in nature and hence the spectral function takes the "universal" form: $\rho_{\rm V}(\omega, \boldsymbol{k}) = (\frac{\omega^2 - k^2}{\omega^2 + D^2 k^4} + 2)\, \chi_{\rm q}\, D\, \omega$, where D is the electrical diffusion coefficient and $\chi_{\rm q} = \frac{1}{T} G^{00}(\tau, \boldsymbol{0})$ is the quark susceptibility. The classical (hydrodynamic) description involves parameters which need to be matched to the microscopic theory, e.g. the electrical conductivity $\sigma_{\rm el}$ defined by $\langle \boldsymbol{J}_{\rm em} \rangle = \sigma_{\rm el} \boldsymbol{E}$. One can obtain the value of the latter from certain limits, as given by the Kubo formulae

$$\sigma_{\rm el} = \chi_{\rm q}\, D = \tfrac{1}{2} \lim_{k \to 0} \rho_{\rm V}(k, \boldsymbol{k})/k = \tfrac{1}{3} \lim_{\omega \to 0} \rho_{\rm V}(\omega, \boldsymbol{0})/\omega\,. \tag{8}$$

For this reason, is has been suggested that $\sigma_{\rm el}$ can be obtained from the appropriate limit of photon and dilepton spectra [44]. For dileptons, the hadronic component is paramount in this limit and in-medium modifications to vector mesons need to be treated accurately [45, 46].

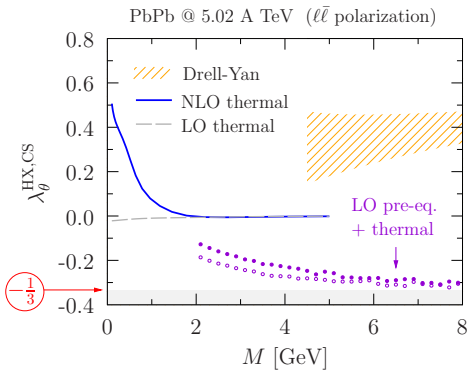

Figure 3. The angular coefficient λ_θ for dileptons in different frames, as a function of invariant mass. Thermal QGP results are from ref. [31] (0–20% centrality), and computed in the helicity frame. The pre-equilibrium and Drell-Yan curves are computed in the Collins-Soper frame, see ref. [30] (0–5% centrality). Both the LO thermal and pre-equilibrium originate from $q\bar{q} \to \gamma^*$. (The open circles have a longer equilibration time than the filled ones.)

4.3 Dilepton polarization

The largest theoretical uncertainty in the succession of models described in sec. 2 is the earliest timespan where the system is highly anisotropic. This far from equilibrium state is difficult to treat rigorously, but impacts the polarization of photons [27]. The angular distribution of dileptons has drawn attention recently, being sensitive to polarization [28], and is usually parametrized (by the leading, frame dependent, coefficients λ_θ and λ_ϕ) by

$$\frac{\mathrm{d}N_{\ell\bar{\ell}}}{\mathrm{d}M\,\mathrm{d}y\,\mathrm{d}\Omega_\ell} \propto 1 + \lambda_\theta \cos^2\theta_\ell + \lambda_\phi \sin^2\theta_\ell \cos 2\phi_\ell + \dots \,, \tag{9}$$

where the angles $\mathrm{d}\Omega_\ell = \mathrm{d}\cos\theta_\ell\,\mathrm{d}\phi_\ell$ refer to one of the final leptons, measured w.r.t. a z-axis chosen conventionally in the virtual photon's rest frame.

In the helicity frame (HX), $\lambda_\theta^{\rm HX} \simeq (\rho_{\rm T} - \rho_{\rm L})/(\rho_{\rm T} + \rho_{\rm L})$ which has been studied in both hadronic [29] and QGP [31] phases. The coefficient $\lambda_\theta^{\rm HX}$ receives a large NLO correction for $M \lesssim 2$ GeV (fig. 3). In the Collins-Soper (CS) frame, $\lambda_\theta^{\rm CS} = 3Q/(\frac{2}{5} - Q)$ where Q is the quadrupole moment of the lepton distribution, which was calculated for the LO pre-equilibrium process $q\bar{q} \to \ell\bar{\ell}$ [30]. When the initial quarks have large longitudinal momenta: $\lambda_\theta^{\rm CS} = 1$ At the other extreme, when the initial quarks carry purely transverse momentum: $\lambda_\theta^{\rm CS} = -\frac{1}{3}$. A sign change of $\lambda_\theta^{\rm CS}$ would thus distinguish these scenarios, see fig. 3.

5 Summary

Electroweak probes are valuable tools for diagnosing the medium in heavy ion collisions. Perturbative and lattice approaches now complement each other, enabling quantitative estimates of non-perturbative effects in emission rates. New insights are being provided by differential observables, like dilepton polarization. Yet some puzzles remain, for example: Measurements of the v_2 for direct photons suggests that current predictions are underestimating thermal photons. This is in tension with fig. 2, where lattice analyses indicate that perturbation theory is overestimating thermal photons. Another questions is the scaling of direct photons with $(\mathrm{d}N_{\rm ch}/\mathrm{d}y)^\alpha$, although there is some disagreement about the value of α on the experimental side [11]. Diverse as the theoretical progress has been, there is still room (and even need) for contributions on both formal aspects and phenomenology.

I am very grateful to F. Arleo, D. Bala, M. Coquet, L. Du, C. Gale, J. Ghiglieri and M. Laine for their valuable comments. The author is supported by the Agence Nationale de la Recherche, under grant ANR-22-CE31-0018.

References

[1] M. Laine and A. Vuorinen, *Basics of Thermal Field Theory*, (Springer, 2016).

[2] J. I. Kapusta and C. Gale, *Finite-Temperature Field Theory*, (Cambridge UP, 2006).
[3] C. Gale, [arXiv:2502.13938].
[4] F. Geurts and R. A. Tripolt, Prog. Part. Nucl. Phys. **128** 104004 (2023).
[5] C. Gale, J. F. Paquet, B. Schenke and C. Shen, Phys. Rev. C **105** 014909 (2022).
[6] O. Massen, *et al.*, Eur. Phys. J. C **85** 388 (2025).
[7] L. Du, EPJ Web Conf. **339** 01016, (2025).
[8] G. Vujanovic, Nucl. Phys. A **1060** 123119 (2025).
[9] J. F. Paquet, PoS **HardProbes2023** 009 (2024).
[10] R. A. Tripolt, Nucl. Phys. A **1005** 121755 (2021).
[11] H. S. Scheid, in these proceedings, [arXiv:2509.26456].
[12] F. Arleo, K. J. Eskola, H. Paukkunen and C. A. Salgado, JHEP **04** 055 (2011).
[13] O. Garcia-Montero, A. Mazeliauskas, P. Plaschke, S. Schlichting, JHEP **03** 053 (2024).
[14] O. Garcia-Montero, P. Plaschke and S. Schlichting, Phys. Rev. D **111** 034036 (2025).
[15] M. Coquet, *et al.*, Phys. Lett. B **821** 136626 (2021).
[16] X. Y. Wu, L. Du, C. Gale and S. Jeon, Phys. Rev. C **110** 054904 (2024).
[17] C. Shen, J. F. Paquet, U. Heinz and C. Gale, Phys. Rev. C **91** 014908 (2015).
[18] G. Vujanovic, *et al.*, Phys. Rev. C **98** 014902 (2018).
[19] G. Vujanovic, *et al.*, Phys. Rev. C **101** 044904 (2020).
[20] X. Y. Wu, in these proceedings, [arXiv:2509.03289].
[21] H. Fujii, K. Itakura, K. Miyachi and C. Nonaka, Phys. Rev. C **106** 034906 (2022).
[22] N. Götz *et al.* [SMASH], Phys. Rev. C **105** 044910 (2022).
[23] A. W. R. Jorge, T. Song, Q. Zhou and E. Bratkovskaya, Phys. Rev. C **111** 064904 (2025).
[24] O. Savchuk, *et al.*, J. Phys. G **50** 125104 (2023).
[25] Z. Nussinov, *et al.*, Phys. Rev. Lett. **135** 101904 (2025).
[26] S. Hauksson, S. Jeon and C. Gale, Phys. Rev. C **97** 014901 (2018).
[27] S. Hauksson and C. Gale, Phys. Rev. C **109** 034902 (2024).
[28] E. Speranza, A. Jaiswal and B. Friman, Phys. Lett. B **782** 395-400 (2018).
[29] F. Seck, *et al.*, Phys. Lett. B **861** 139267 (2025).
[30] M. Coquet, *et al.*, Phys. Rev. Lett. **132** 232301 (2024).
[31] X. Y. Wu, *et al.*, Phys. Rev. Lett. **134** 242301 (2025).
[32] A. Francis, PoS **QCHSC24** 173 (2025).
[33] H. T. Ding, *et al.*, Phys. Rev. D **83** 034504 (2011).
[34] J. Ghiglieri, O. Kaczmarek, M. Laine and F. Meyer, Phys. Rev. D **94** 016005 (2016).
[35] M. Cè, *et al.*, Phys. Rev. D **102** 091501 (2020).
[36] M. Cè, *et al.*, Phys. Rev. D **106** 054501 (2022).
[37] S. Ali *et al.* [HotQCD], Phys. Rev. D **110** 5 (2024).
[38] G. Jackson and M. Laine, JHEP **11** 144 (2019).
[39] H. B. Meyer, Eur. Phys. J. A **54** 192 (2018).
[40] M. Cè, *et al.*, Phys. Rev. D **109** 014507 (2024).
[41] J. Churchill, *et al.*, Phys. Rev. Lett. **132** 172301 (2024).
[42] J. Churchill, *et al.*, Phys. Rev. C **109** 044915 (2024).
[43] R. Góes-Hirayama, in these proceedings, [arXiv:2510.02862].
[44] S. Floerchinger, C. Gebhardt and K. Reygers, Phys. Lett. B **837** 137647 (2023).
[45] R. Rapp, Phys. Rev. C **110** 054909 (2024).
[46] J. Atchison, Y. Han and F. Geurts, Phys. Lett. B **858** 139024 (2024) and these proceedings.
[47] L. Du, Phys. Lett. B **861** 139270 (2025).